Original Article

Proc IMechE Part D:
J Automobile Engineering
1–14

DOI: 10.1177/0954407016672775
pid.sagepub.com

A unified approach to the kinematic synthesis of five-link, four-link, and double-wishbone suspension mechanisms with rack-and-pinion steering control

P A Simionescu

Abstract

This paper presents a unified approach to the problem of dimensional synthesis of the five-link, four-link, and three-link (double-wishbone) suspension mechanisms with a rack-and-pinion steering input. In a simplified approach, the guiding links are assumed to be removed from their joints, allowing the wheel to be exactly driven through a number of prescribed jounce–rebound and steering positions during the kinematic synthesis process. Alternatively, the tie rod is maintained in place, and the rack length and the lengths of the remaining four guiding links are allowed to vary. An optimization problem based on the aggregated change in distance between the released ball joints evaluated in the aforementioned positions is then defined. By prescribing to the wheel a jounce–rebound motion only, rear-suspension mechanisms of the five-link, four-link, and three-link types can be conveniently synthesized by following the same procedure. Several solutions obtained through synthesis are then analyzed for their changes in steering error, recessional wheel motion, wheel track, toe angle and camber angle, showing very promising results. Additionally, a comprehensive review of nearly 150 publications relevant to the suspension design of automobiles is provided in the paper.

Keywords

Steering and suspension, rigid-body guidance, constraint equations, kinematic synthesis, optimization

Date received: 7 March 2016; accepted: 5 September 2016

Introduction

The independent suspensions of automobiles are complex spatial mechanisms tuned to fulfil the multiple requirements imposed on the motion of the wheels relative to the chassis, and of the chassis relative to the ground, during acceleration, braking and cornering maneuvers.[1–5] To improve their ride and handling characteristics, new suspension designs of the multi-link type have been proposed and implemented in production vehicles in the last three decades.

The five-link suspension mechanism was first applied by Daimler–Benz to the rear wheels of the C111 experimental model,[6] and then in the 1980s to the W201 (190/190 E) and W124 (200 D/300 E) series.[7, 8] Five-link (5SS)[5–24] and four-link (3SS-RS)[25–31] (also known as quadra-link) mechanisms have been since implemented by car manufacturers in both the rear suspension[5–9, 13–25, 27–31] and the front suspension.[10–12, 15, 26, 27] Numerous reports dealing with their synthesis[11–13, 32–60] and analysis[37, 42, 51, 52, 57, 61–90] and of the equivalent three-dimensional rigid-body guidance linkages (with or without considering the effect of joint compliances) have been published around world. A substantial amount of literature also exists on the design and analysis of the more commonly used double-wishbone suspension (also known as the AA suspension), and of its short–long A (SLA) version, as well as on the kinematic synthesis of the corresponding RSSR-SS and RSSR-RRS linkages.[91–115] Other than their traditional application to passenger cars,[116–121] double-wishbone suspensions

Texas A&M University Corpus Christi, Corpus Christi, Texas, TX, USA

Corresponding author:
Petru A Simionescu, Texas A&M University Corpus Christi, 6300 Ocean Drive, Corpus Christi, TX 78412, USA
Email: pa.simionescu@tamucc.edu

have found increasing use in motor coaches, trucks, agricultural tractors, and off-road vehicles.[115, 122–125] There are also reports on three-link suspension configurations that depart from what it is commonly assumed to be a double-wishbone mechanism,[129–131] which are also termed multi-link suspensions. Suspension mechanisms with both serial and parallel combinations of links and joints have also been proposed and implemented in the front axle and the rear axle of automobiles.[122–143] Such arrangements require individualized treatment for their kinematic synthesis and are not considered in this paper.

As pointed out elsewhere,[67, 75, 78] double-wishbone suspensions can be assumed to be 5SS linkages having four of the outboard joints two-by-two coincident. Similarly, quadra-link suspensions can be considered to be particular embodiments of the 5SS arrangement where two of the joints attached to the wheel carrier coincide,[78] i.e. either a top pair or a bottom pair.

Some of the above-cited papers report on the design of multi-link[40, 57, 58] and double- wishbone[100, 103, 105, 106, 107, 109] front-suspension mechanisms through repeated analysis and the use of simulation software or computer algebra systems. Graphical[1–5, 10–12], analytical and numerical approaches[26, 48, 50, 56, 97, 101, 102, 113] to five-link, four-link, and three-link front suspension kinematic synthesis are available to the interested reader, but these methods appear to be difficult to implement and are rarely accompanied by clearly illustrated numerical examples. Publications on the dimensional synthesis of the 5SS, RSSR-SS and RSSR-RRS parallel mechanism for rigid-body guidance (also known to kinematicians as "motion generators") or for path generation have reported the use of the spatial Burmester theory,[32–35, 38, 39] optimization techniques,[37, 43, 91, 92, 95] or precision points.[36, 93, 94]

The method proposed by the present author and coworkers[42, 51] is extended here for the cases where the wheel receives an additional steering input. As the examples provided in the second part of the paper show, promising results were obtained in the case of multi-link suspensions equipped with either a trailing steering rack or a leading steering rack. Additionally, very good solutions of four-link and double-wishbone front-suspension mechanisms were identified using the same approach.

Problem formulation

Figure 1 is a schematic diagram of a five-link suspension with rack-and-pinion steering control, where the reference frame Oxyz is attached to the vehicle and the reference frame O$'x'y'z'$ is attached to the wheel. For simplicity, it is assumed that, in the neutral position, these two reference frames are parallel. Also shown in Figure 1 are the wheel-print center S, the virtual steering axis N_1N_2 (which intersects the road surface at point N), and the steering angle θ_L measured from the neutral position of the wheel, oriented as shown.

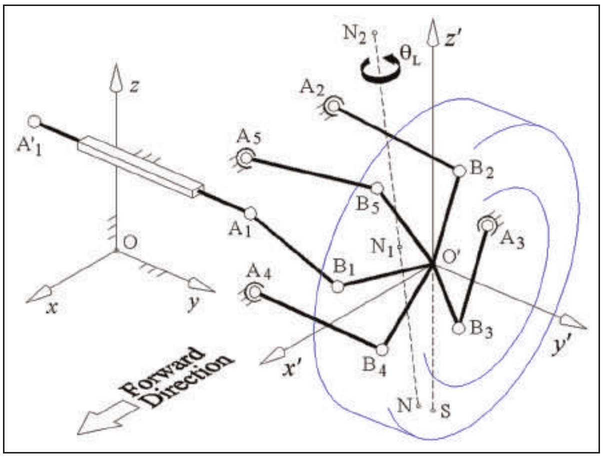

Figure 1. Five-link suspension mechanism with leading rack-and-pinion steering control.

With the notation in Figure 1, the four-link and double-wishbone mechanisms can be easily modeled by imposing that the ball joint centers B_4 and B_5 or/and B_2 and B_3 coincide.

The requirements for correlated steering and jounce–rebound motion with minimum toe, camber and wheel track changes are formulated as a minimization problem of 30 variables, i.e. the x, y and z coordinates of ball joints $A_1, \ldots, A_5$ relative to the chassis, and the x', y' and z' coordinates of ball joints $B_1, \ldots, B_5$ relative to the wheel carrier. In the case of the quadra-link and double-wishbone mechanisms, the numbers of variables are reduced to 27 and 24 respectively. It should be noted that, in a more general formulation, the lock-to-lock travel of the steering rack can also be considered to be a design variable of the continuous or discrete type, although, as explained by Simionescu and Smith,[144] the desired rack travel can be achieved through proper scaling.

The prescribed wheel motion in the rigid-body-guidance synthesis problem of the suspension mechanism is assumed to have the following two components:

(a) a pure vertical translation (the jounce–rebound motion) corresponding to point O$'$ moving by a disance $\pm\Delta z_{O'}$ from its reference position;
(b) a rotation θ_L of the wheel carrier about the axis N_1N_2 (the steering motion).

These two combined motions are controlled in n_z discrete position and n_θ discrete position respectively, as shown in Figure 2.

Two approaches to the kinematic synthesis problem will be described next:

Approach 1. In this approach links A_iB_i ($i = 1, \ldots, 5$) are considered to be removed from their joints, allowing the wheel to be exactly driven through the predefined positions shown in Figure 2, and an optimization

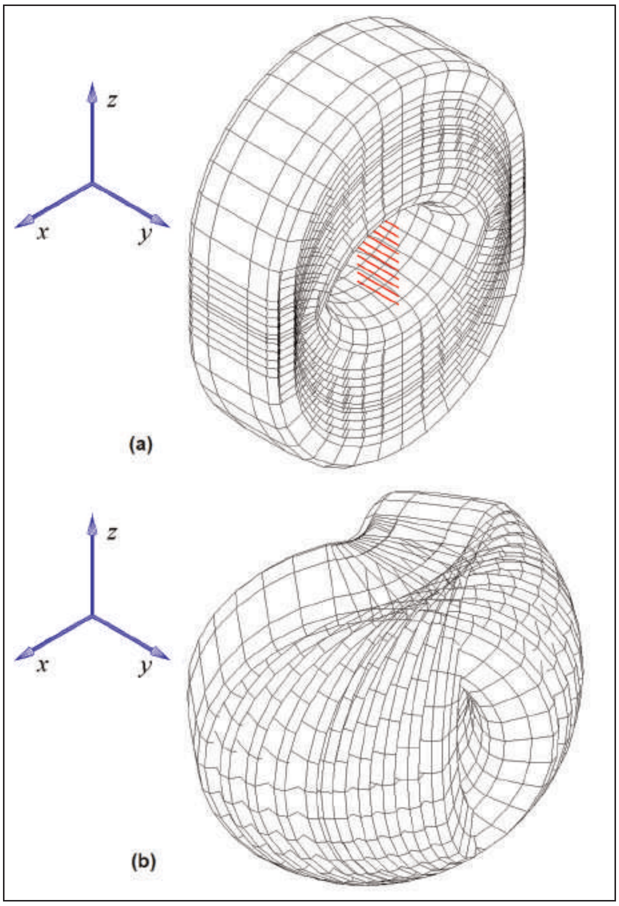

Figure 2. Prescribed wheel motion in the synthesis problem discussed in the paper which consists of (a) pure vertical displacements, combined with (b) rotated positions about an imposed virtual steering axis N_1N_2.

problem is defined as explained below with reference to equation (2). The y displacement of the rack end A_1 (measured from the zero position to its lock-to-lock positions $\pm\Delta y_{A_1}$) is assumed to be linearly correlated to the steering angle θ_L of the wheel according to the graph in Figure 3. The maximum inner steering angle $\theta_{I\ max}$ is limited by the angular capability of the constant-velocity axle, while the maximum outer steering angle $\theta_{O\ max}$ results from the Ackermann geometry[145, 146]:

$$\theta_O = \arctan\left[\frac{1}{\cot\theta_I + 1/(W_b/W_t)}\right] \tag{1}$$

where W_b is the wheelbase and W_t is the wheel track of the vehicle.

Approach 2. In this approach, the tie rod A_1B_1 is maintained in place and the rack length A_1A_1' is allowed to vary from its reference value l_R, as the wheel is driven through the imposed jounce–rebound positions (Figure 2(a)), and from the maximum left-steer position to the maximum right-steer position, correlated according to the dashed curve in Figure 3. The remaining link lengths A_iB_i ($i = 2, \ldots, 5$) are also allowed to change, in a similar way to *Approach 1*, and an optimization problem is defined as explained below with reference to equation (3). The y coordinates of the ball joints A_1 and A_1' required to calculate the variable rack length A_1A_1' caused by wheel steering are determined as the intersection between the line of sliding of the rack, and a sphere centered at B_1 and of radius A_1B_1.

It should be noted that, in both *Approach 1* and *Approach 2*, there is no need to model the right-side suspension separately, as this is simply the mirror image of the left-side suspension shown in Figure 1.

In the case of *Approach 1*, the objective function to be minimized is defined as the maximum norm of the change in the distance between the homologous ball-joint centers A_i and B_i with $i = 1, \ldots, 5$, according to

$$F_1\left(x_{A_i}, y_{A_i}, z_{A_i}, x'_{B_i}, y'_{B_i}, z'_{B_i}\right)_{i=1,\ldots,5} = \max\left(w_i\left|l_i - (A_iB_i)_j\right|, w_i\left|l_i - (A_iB_i)_k\right|\right) \tag{2}$$

For *Approach 2*, the corresponding objective function was set equal to the maximum norm of the change in the distance between the rack-end ball joints A_1 and A_1' and the ball-joint centers A_i and B_i with $i = 2, \ldots, 5$ (see Figure 1)

$$\begin{aligned} F_2\left(x_{A_i}, y_{A_i}, z_{A_i}, x'_{B_i}, y'_{B_i}, z'_{B_i}\right)_{i=1,\ldots,5} &= \max\left(w_1\left|l_R - (A_1A_1')_j\right|, l_R - (A_1A_1')_k,\right. \\ &\left. w_i\left|l_i - (A_iB_i)_j\right|, w_i\left|l_i - (A_iB_i)_k\right|\right) \end{aligned} \tag{3}$$

In both equation (2) and equation (3), it is assumed that $j = 1, \ldots, n_z$ and $k = 1, \ldots, n_\theta$, where n_z is the number of imposed vertical displacements and n_θ is the number of imposed steering positions of the wheel (Figure 2). The weighting coefficients w_i were added to allow the designer to control the steering error contribution to the values of the objective functions F_1 and F_2 versus the contributions of the variations in wheel track or camber angle (see the third section of the paper for details).

The guiding link lengths l_1 to l_5 are determined as the distances between the joints A_i and B_i for the suspension in its neutral position, while the variable distances between the joints A_i and B_i in a current position of the wheel carrier are

$$(A_iB_i)_{j,k} = \sqrt{\left(x_{A_ij,k} - x_{B_ij,k}\right)^2 + \left(y_{A_ij,k} - y_{B_ij,k}\right)^2 + \left(z_{A_ij,k} - z_{B_ij,k}\right)^2} \tag{4}$$

where the coordinates x, y, and z are specified relative to the fixed frame Oxyz, as explained next.

For the jounce–rebound displacements of the wheel (Figure 2(a)), the 3D transformations applied are

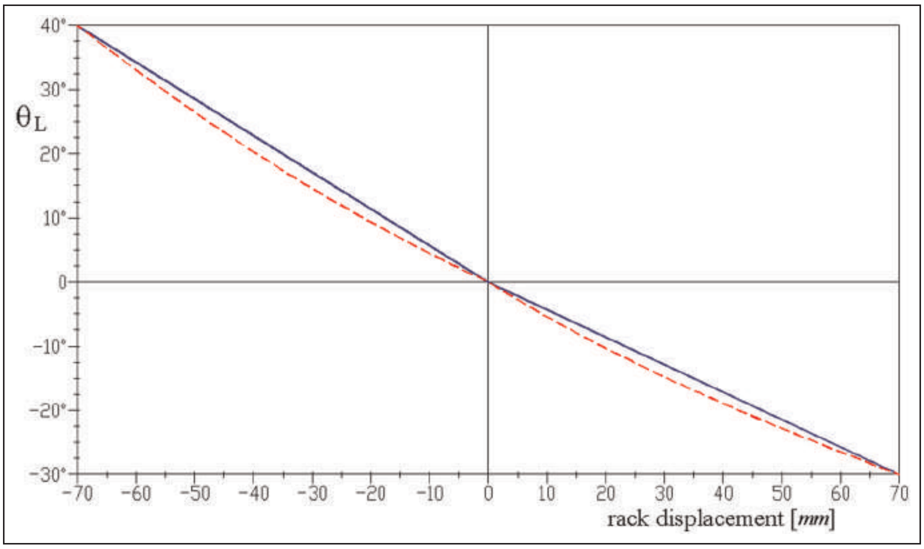

Figure 3. Linear (solid curve) and Ackermann (dashed curve) steering correlations between the rack displacement and the steering angle θ_L of the left wheel, for $\theta_{I\,max}$ = 40°, W_b/W_t = 1.85, and Δy_{A_1} = ±70 mm.

$$\begin{bmatrix} x_{B_ij} \\ y_{B_ij} \\ z_{B_ij} \end{bmatrix}_{Oxyz} = \begin{bmatrix} x'_{B_i} \\ y'_{B_i} \\ z'_{B_i} \end{bmatrix}_{O'x'y'z'} + \begin{bmatrix} x_{O'j} \\ y_{O'j} \\ z_{O'j} \end{bmatrix}_{Oxyz} \tag{5}$$

while, in the case of the steering positions (Figure 2(b)), the coordinates of the ball-joint centers $B_1, \ldots, B_5$ are determined as screw displacements[147] according to

$$\begin{bmatrix} x_{B_ik} \\ y_{B_ik} \\ z_{B_ik} \end{bmatrix}_{Oxyz} = \left[R_{\theta\, u_x u_y u_z}\right] \begin{bmatrix} x'_{B_i} - x'_{N_1} \\ y'_{B_i} - y'_{N_1} \\ z'_{B_i} - z'_{N_1} \end{bmatrix} + \begin{bmatrix} x'_{N_1} \\ y'_{N_1} \\ z'_{N_1} \end{bmatrix}_{O'x'y'z'} + \begin{bmatrix} x_{O'j} \\ y_{O'j} \\ z_{O'j} \end{bmatrix}_{Oxyz} \tag{6}$$

where

$$\left[R_{\theta\, u_x u_y u_z}\right] = \begin{bmatrix} (1-c)u_x^2 + c & (1-c)u_x u_y - s u_z & (1-c)u_x u_z + s u_y \\ (1-c)u_x u_y + s u_z & (1-c)u_y^2 + c & (1-c)u_y u_z - s u_x \\ (1-c)u_x u_z + s u_y & (1-c)u_y u_z + s u_x & (1-c)u_z^2 + c \end{bmatrix} \tag{7}$$

with

$$u_x = \frac{x'_{N_2} - x'_{N_1}}{|N_1N_2|}, \quad u_y = \frac{y'_{N_2} - y'_{N_1}}{|N_1N_2|}, \quad u_z = \frac{z'_{N_2} - z'_{N_1}}{|N_1N_2|} \tag{8}$$

and with $c = \cos\theta_L$ and $s = \sin\theta_L$.

The variable y coordinate of the rack end A_1 occurring in *Approach 2* results as the intersection between the sphere centered at B_1 and of radius l_1, and the line of sliding of the rack with $x = x_{A_1}$ and $z = z_{A_1}$ i.e.

$$y_{A_1} = y_{B_1} - \sqrt{A_1B_1^2 - (x_{A_1} - x_{B_1})^2 - (z_{A_1} - z_{B_1})^2} \tag{9}$$

The objective functions F_1 and F_2 in equations (2) and (3) must be constrained by the allowable locations of the ball joints on the chassis and on the wheel carrier (Figure 4). First, side constraints must be imposed in order to avoid convergence to unpractical solutions with links that are too long. Additional geometric constraints must be prescribed so that the ball joints B_i ($i = 1, \ldots, 5$) remain within the available space limited by the wheel rim, the wheel hub, and the inboard side of the tire, a case explained in more detail by Simononescu et al.[146] Also imposed is the minimum allowable distance between two neighboring ball joints B, and between the rack joints A_1 and A'_1 in the case of central-outrigger steering-rack arrangements.[147] This minimum distance was limited to 2.5 times the diameter of the ball joints $A_1, \ldots, A_5$ and $B_1, \ldots, B_5$, which are all assumed to be identical.

Numerical results

The objective functions F_1 and F_2 subjected to the above-listed constraints were minimized using a modified Nelder–Mead simplex optimization algorithm, where all the design variables x_{A_i}, y_{A_i}, z_{A_i}, x_{B_i}, y_{B_i}, and z_{B_i} ($i = 1, \ldots, 5$) are rounded to the nearest 0.5 mm[148]. The following parameters were specified as the inputs to these two optimization problems.

1. The wheel rebound limits and the wheel jounce limits (±75 mm) measured from the static position of point O′.
2. The lock-to-lock travel of the steering rack ($y_{A_1max} - y_{A_1min}$ = 140 mm).
3. The maximum inner steering angle ($\theta_{I\,max}$ = 40°) and (for the objective function F_1 only) and the outer steering angle ($\theta_{O\,max}$ = 30°).

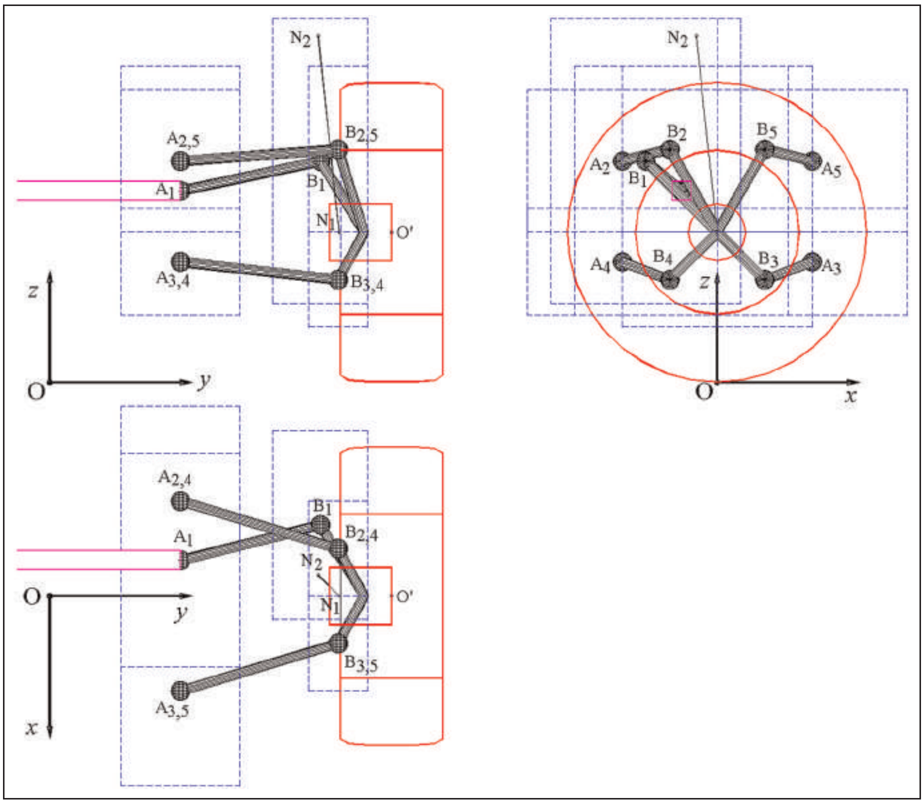

Figure 4. Side constraints to the design variables x_{A_i}, y_{A_i}, z_{A_i}, x_{B_i}, y_{B_i}, and z_{B_i} ($i = 1, \ldots, 5$) represented as dashed rectangles. To obtain the central-takeoff steering-rack solutions, the side constraints of the design variable y_{A_1} should be set close to zero, i.e. in the reference position the ball joint A_1 should be near the axis of the vehicle.

4. In the case of the objective function F_2, the wheel-base over the wheel-track ratio required to calculate the correlated steering angles using equation (1) must also be specified (i.e. $W_b/W_t = 1.85$).
5. The number of jounce–rebound positions ($n_z = 20$).
6. The number of lock-to-lock steering positions ($n_\theta = 20$). When synthesizing a rear-wheel suspension mechanism, n_θ must be set to 1.
7. The weighting coefficients in equations (2) and (3). These were $w_2 = w_3 = w_4 = w_5 = 1.0$ and $w_1 = 1.25$ for the imposed steering positions and $w_1 = 1.15$ for the imposed jounce–rebound positions.
8. The radius of the wheel which is equal to the distance O′S in Figure 1 (i.e. O′S = 315 mm).
9. The inner radius of the wheel rim (160 mm).
10. The wheel hub assumed to be a cylinder starting at the center O′ of the wheel and extending inwards with a radius of 60 mm and a length of 115 mm (see Figures 1 and 4).
11. The radii of the ball joints $A_1, \ldots, A_5$ and $B_1, \ldots, B_5$ (20 mm).
12. The coordinates of the point O′ relative to the Oxyz reference frame for the wheel in its neutral position (0, 720, 315).
13. The side constraints of the coordinates of the centers of the ball joints $A_1, \ldots, A_5$ relative to the Oxyz reference frame and of the ball joints $B_1, \ldots, B_5$ relative to the O′$x'y'z'$ reference frame (see Table 1).

In the case of the upper A-arm quadra-link suspension mechanism, the ball joints B_2 and B_5 must coincide (i.e. the design variables x'_{B_5}, y'_{B_5}, and $z'_{B_5}$are suppressed), and the search domain of variable x'_{B_2} is changed to [−150, 150] mm. After first swapping the ball joints B_2 and B_5, and the ball joints B_3 and B_3, the same modifications are applied when synthesizing a lower A-arm quadra-link suspension.

Finally, when synthesizing a three-link suspension, the ball joints B_2 and B_5 and the ball joints B_3 and B_4 are assumed to be coincident (i.e. the design variables x'_{B_5}, y'_{B_5}, z'_{B_5},x'_{B_4}, y'_{B_4}, and z'_{B_4} are suppressed), and the ranges of the design variables x'_{B_2} and $x'_{B_3}$are changed to [−150, 150] mm.

The kinematic parameters of the best five-link, four-link, and double-wishbone suspension mechanisms obtained through synthesis (both standard and central-takeoff rack) are summarized in Tables 2 to 5. Their performances are shown for comparison in Figures 5 to 11. Of these, Figure 5 shows the steering-angle correlation of these four solutions compared with the Ackermann law. Figure 6 shows plots of the change x_S in the recessional wheel motion and the change y_S in the wheel track, while Figure 7 shows the variations in the toe angle and the camber angle versus the vertical motion of the wheel.

The steering angles and the toe angles used to generate Figures 5 and 7(a) were determined as the angle between the fixed axis Oy and the projection on the

Table 1. Search domains of the design variables x_{A_i}, y_{A_i}, z_{A_i}, x'_{B_i}, y'_{B_i} and z'_{B_i} with $i = 1, \ldots, 5$ for the full five-link suspension mechanism (the values are given in millimeters).

$-300 \leqslant x_{A_1} \leqslant 100$ (for the trailing rack)	$150 \leqslant y_{A_1} \leqslant 400$ (for the standard steering rack)	$125 \leqslant z_{A_1} \leqslant 650$
$-100 \leqslant x_{A_1} \leqslant 300$ (for the leading rack)	$0 \leqslant y_{A_1} \leqslant 50$ (for the central outrigger steering rack)	
$-400 \leqslant x_{A_2} \leqslant 0$	$150 \leqslant y_{A_2} \leqslant 400$	$300 \leqslant z_{A_2} \leqslant 600$
$0 \leqslant x_{A_3} \leqslant 400$	$150 \leqslant y_{A_3} \leqslant 400$	$125 \leqslant z_{A_3} \leqslant 350$
$-400 \leqslant x_{A_4} \leqslant 0$	$150 \leqslant y_{A_4} \leqslant 400$	$125 \leqslant z_{A_4} \leqslant 350$
$0 \leqslant x_{A_5} \leqslant 400$	$150 \leqslant y_{A_5} \leqslant 400$	$300 \leqslant z_{A_5} \leqslant 600$
$-350 \leqslant x'_{B_1} \leqslant 50$	$-250 \leqslant y'_{B_1} \leqslant -50$	$-150 \leqslant z'_{B_1} \leqslant 450$
$-200 \leqslant x'_{B_2} \leqslant 0$	$-175 \leqslant y'_{B_2} \leqslant -50$	$0 \leqslant z'_{B_2} \leqslant 350$
$0 \leqslant x'_{B_3} \leqslant 200$	$-175 \leqslant y'_{B_3} \leqslant -50$	$-200 \leqslant z'_{B_3} \leqslant 0$
$-200 \leqslant x'_{B_4} \leqslant 0$	$-175 \leqslant y'_{B_4} \leqslant -50$	$-200 \leqslant z'_{B_4} \leqslant 0$
$0 \leqslant x'_{B_5} \leqslant 200$	$-175 \leqslant y'_{B_5} \leqslant -50$	$0 \leqslant z'_{B_5} \leqslant 350$

Table 2. Five-link suspension mechanism solution obtained by minimizing the objective function F_1.

	Values of the design variables $i = 1, \ldots, 5$				
	$i = 1$	$i = 2$	$i = 3$	$i = 4$	$i = 5$
x_{A_i} (mm)	−265.5	−314.0	360.5	−242.5	237.5
y_{A_i} (mm)	358.5	233.5	286.0	283.0	241.5
z_{A_i} (mm)	360.5	574.0	225.0	218.5	292.5
x'_{B_i} (mm)	−68.5	−53.0	49.5	−17.5	5.5
y'_{B_i} (mm)	−50.0	−149.0	−142.5	−109.5	−152.5
z'_{B_i} (mm)	45.5	254.0	−113.0	−79.0	170.5
l_i (mm)	368.57	426.68	426.87	399.43	400.19

Table 3. Four-link suspension mechanism solution obtained by minimizing the objective function F_2.

	Values of the design variables $i = 1, \ldots, 5$				
	$i = 1$	$i = 2$	$i = 3$	$i = 4$	$i = 5$
x_{A_i} (mm)	45.5	−356.5	99.5	−392.5	177.0
y_{A_i} (mm)	229.5	306.0	163.5	347.5	272.5
z_{A_i} (mm)	468.5	462.0	184.0	229.5	454.5
x'_{B_i} (mm)	−131.5	−10.5	1.5	−16.5	(−10.5)
y'_{B_i} (mm)	−137.5	−122.0	−55.5	−122.5	(−122.0)
z'_{B_i} (mm)	153.5	139.5	−119.0	−79.0	(139.5)
l_i (mm)	394.89	452.81	510.64	451.57	375.64

Table 4. Standard three-link suspension mechanism solution obtained by minimizing the objective function F_1.

	Values of the design variables $i = 1, \ldots, 5$				
	$i = 1$	$i = 2$	$i = 3$	$i = 4$	$i = 5$
x_{A_i} (mm)	−224.0	−114.5	300.0	−396.5	243.0
y_{A_i} (mm)	150.0	151.0	214.0	312.5	230.0
z_{A_i} (mm)	302.5	440.5	211.0	203.5	441.0
x'_{B_i} (mm)	−108.0	−19.0	9.5	(9.5)	(−19.0)
y'_{B_i} (mm)	−50.0	−108.5	−86.5	(−86.5)	(−108.5)
z'_{B_i} (mm)	−12.5	126.0	−107.5	(−107.5)	(126.0)
l_i (mm)	532.78	470.30	510.28	517.58	462.80

Table 5. Central-outrigger three-link suspension mechanism solution obtained by minimizing the objective function F_2.

	Values of the design variables i = 1, ..., 5				
	i = 1	i = 2	i = 3	i = 4	i = 5
x_{A_i} (mm)	−11.5	−400.0	420.5	−204.5	398.5
y_{A_i} (mm)	32.0	249.0	154.0	150.0	261.5
z_{A_i} (mm)	301.5	420.5	204.5	204.0	420.5
x'_{B_i} (mm)	−126.5	−12.5	8.0	(8.0)	(−12.5)
y'_{B_i} (mm)	−90.5	−113.5	−87.5	(−87.5)	(−113.5)
z'_{B_i} (mm)	−13.5	105.5	−111.0	(−111.0)	(105.5)
l_i (mm)	608.47	527.22	536.89	527.22	536.61

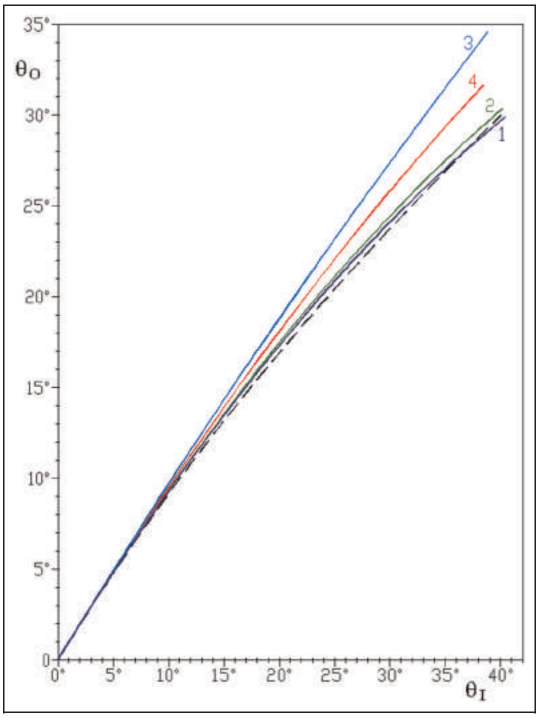

Figure 5. Correlations of the steering angle of the wheel of the five-link (curve 5), four-link (curve 4), standard double-wishbone (curve 3), and central-outrigger double-wishbone (curve 3′) optimum suspension mechanism solutions, overlapping the Ackermann law results (dashed curve).

horizontal plane of the O′y' axis attached to the wheel. Similarly, the camber angle used to generate Figure 7(b) was determined as the angle between the fixed axis Oy and the projection on the vertical plane Oyz of the O′z' axis attached to the wheel.

Figures 8 to 11 show the same four suspension mechanism solutions in their limit positions. Animated GIF files of the same are available for download from the author's ResearchGate page.[149] Additional solutions obtained through synthesis accompanied by animated GIF files are available with reference.[148]

After numerous experiments, it was found that an optimum solution is influenced by the following prescribed parameters: the rack maximum displacement; the jounce–rebound limits; the weighting coefficients w_1 to w_5 adopted in equations (2) and (3); the maximum steering angle $\theta_{I\ max}$ of the inner wheel. Therefore, no claim is made that the numerical solutions reported in this paper are the absolute best obtainable using the synthesis *Approaches* 1 and 2 introduced earlier. The ultimate decision upon the geometric configuration of the mechanism to be implemented in a real vehicle should be based on detailed multi-body dynamic simulations, where the properties of the springs, tires, joint compliances and inertia properties of the vehicle are all taken into account.

Conclusions

The problem of synthesizing five-link, four-link, and three-link (double-wishbone) suspension mechanisms with a rack-and-pinion steering input was conveniently formulated as a single-objective optimization problem, which does not require a complete kinematic analysis of the mechanism at each step of the optimum search. The alternative would have been to combine the changes in the steering error, the recessional wheel motion, the wheel track, the toe angle and the camber angle in a multi-criterion optimization problem, which is substantially more difficult to formulate.

In a first approach, the guiding links of the wheel were assumed to be removed from their joints, allowing the wheel to be exactly driven through a number of prescribed jounce–rebound and steering positions. In a second approach, the tie rod was maintained in place, and instead the rack length was allowed to vary. Scalar objective functions (denoted F_1 and F_2 in this paper), based on the change in the distance between the released ball joints evaluated in the imposed positions were then defined. Another innovation of this paper was that the link lengths and the ball-joint coordinates were rounded to practical values right from within these objective functions, instead of post-synthesis. Some of the most promising solutions obtained were analyzed for performance, and animations of these simulations are available online from the author's ResearchGate page.[149] Either by scaling the numerical solutions presented in this paper or by repeating the optimization problems described for different wheel sizes and rack travels, automotive engineers can design their own front-suspension mechanisms to fit a given

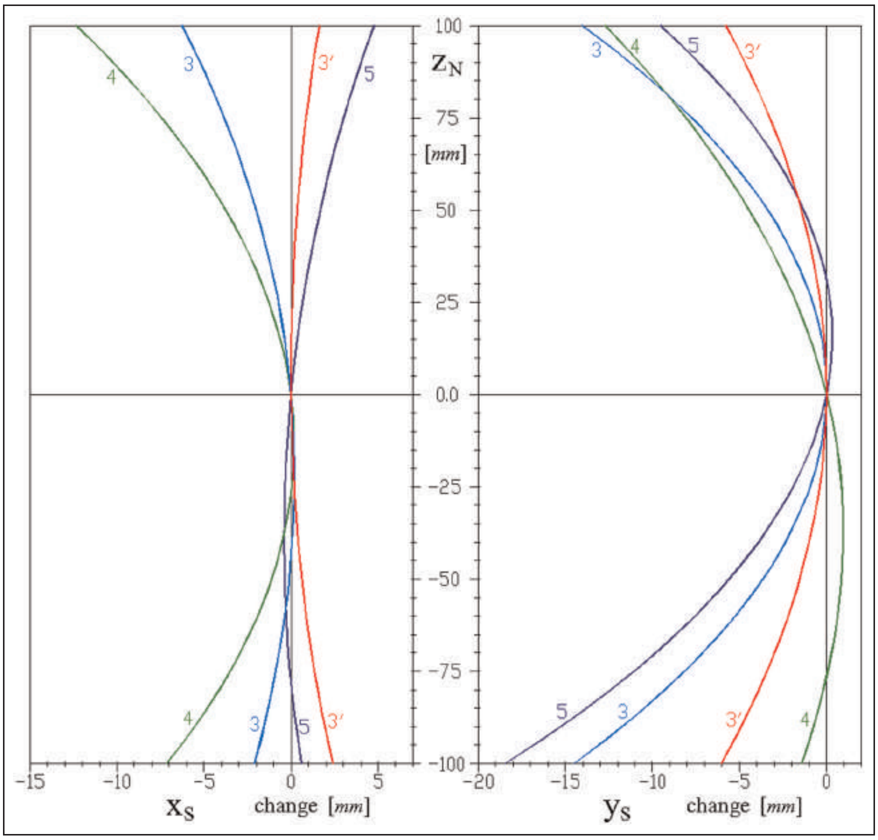

Figure 6. Changes in (a) the recessional wheel motion and (b) the wheel track during the jounce and the rebound of the same suspension mechanisms as in Figure 5.

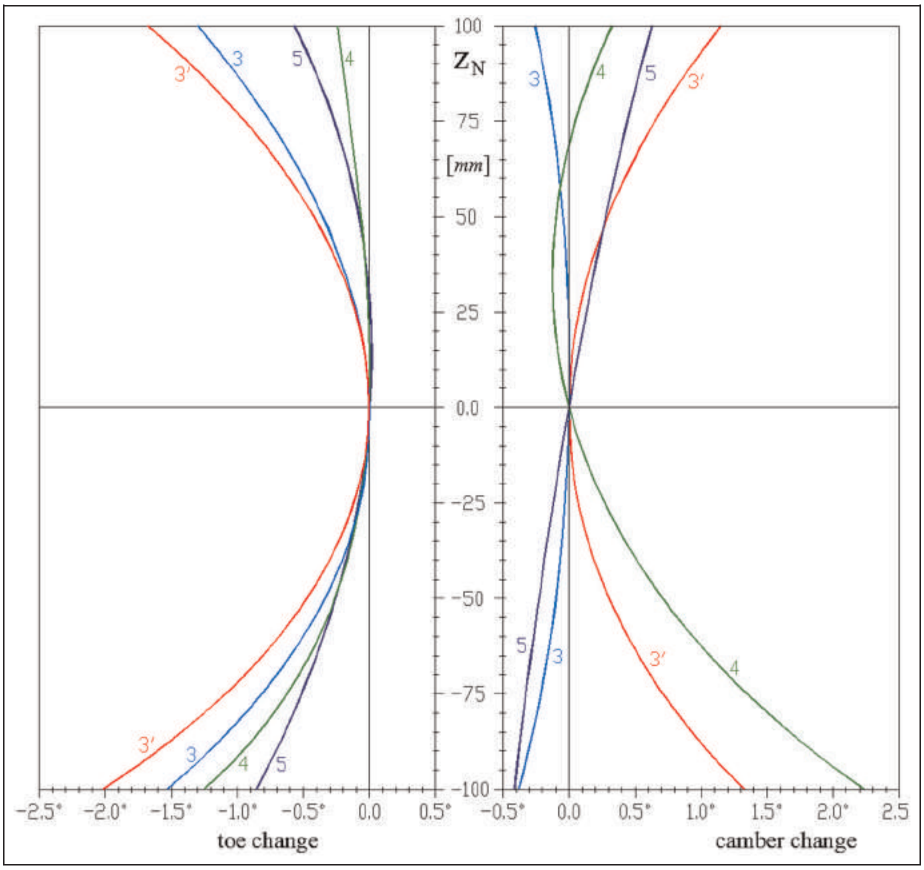

Figure 7. Variations in (a) the toe angle and (b) the camber angle during the jounce and the rebound of the same suspension mechanisms as in Figure 5.

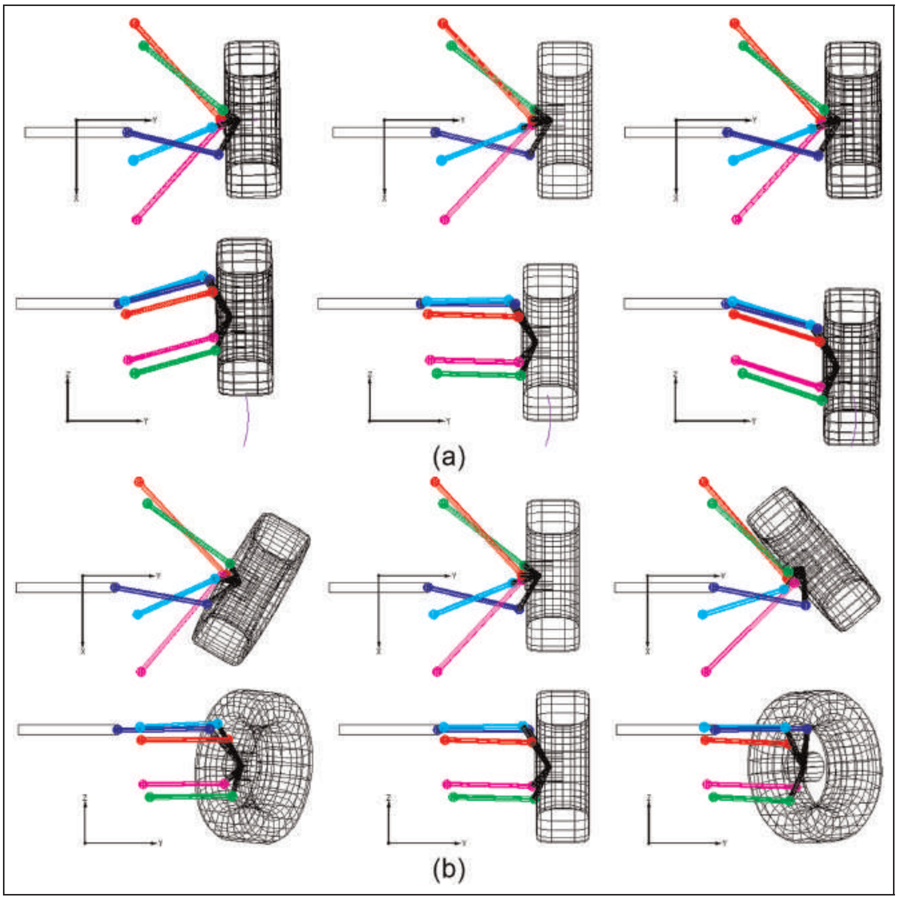

Figure 8. The optimum five-link suspension mechanism in Table 2 showing the limits of (a) the jounce–rebound and (b) the steering positions. See also the animation files Fig08-1.GIF, Fig08-2.GIF, Fig08-3.GIF, and Fig08-4.GIF posted on ResearchGate.[149]

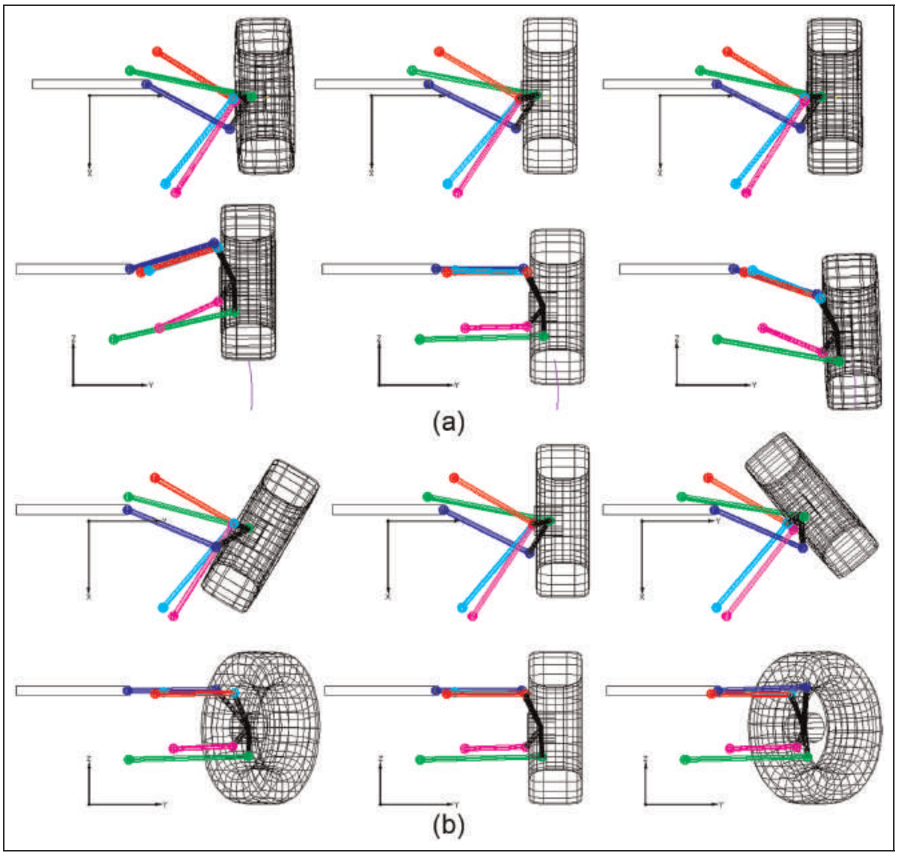

Figure 9. The optimum quadra-link suspension mechanism in Table 3 showing the limits of (a) the jounce–rebound and (b) the steering positions. See also the animation files Fig09-1.GIF, Fig09-2.GIF, Fig09-3.GIF, and Fig09-4.GIF posted on ResearchGate.[149]

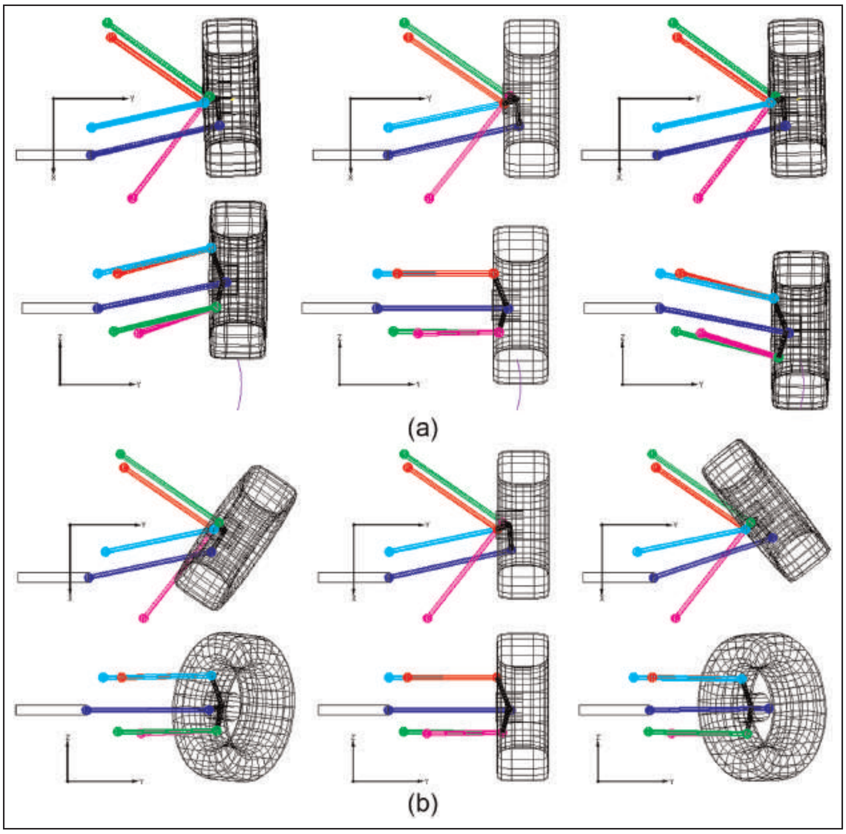

Figure 10. The optimum double-wishbone suspension mechanism in Table 4 showing the limits of (a) the jounce–rebound and (b) the steering positions. See also the animation files Fig10-1.GIF, Fig10-2.GIF, Fig10-3.GIF, and Fig10-4.GIF posted on ResearchGate.[149]

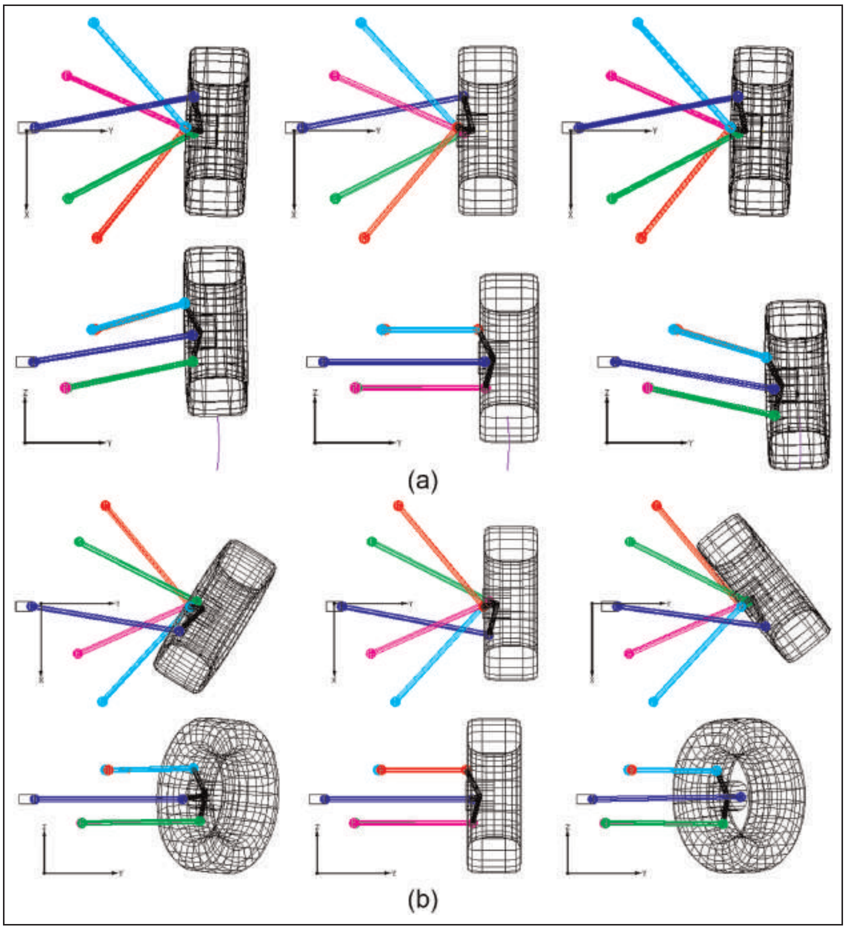

Figure 11. The optimum double-wishbone suspension mechanism with the central-outrigger steering rack in Table 5 showing the limits of (a) the jounce–rebound and (b) the steering positions. See also the animation files Fig11-1.GIF, Fig11-2.GIF, Fig11-3.GIF, and Fig11-4.GIF posted on ResearchGate.[149]

vehicle. It is emphasized that multi-body simulations are necessary ultimately to validate a kinematic solution obtained, and before expensive prototype building and testing are performed.

Funding

The author received no financial support for the research, authorship, and/or publication of this article.

Declaration of conflicting interest

The author declared no potential conflicts of interest with respect to the research, authorship, and/or publication of this article.

References

1. Dixon JC. *Tires, suspension and handling*. Warrendale, Pennsylvania: SAE International, 1996.
2. Reimpell J, Stoll H and Betzler JW. *Automotive chassis: engineering principles*. Oxford: Butterworth–Heinemann, 2001.
3. Matschinsky W. *Radführungen der Straßenfahrzeuge: Kinematik, Elasto-Kinematik und Konstruktion*. Berlin: Springer, 2007.
4. Stockmar J. *Design of automotive suspension systems*, Vienna: Institut für Fahrzeugantriebe und Automobiltechnik, Technische Universität Wien, 2013.
5. Bastow D, Howard G and Whitehead JP. *Car suspension and handling*. Warrendale, Pennsylvania: SAE International, 2014.
6. Bastow D. Suspension and steering. *Auto Engr* 1970; 8: 217–231.
7. Von der Ohe M. *Independent wheel suspension*. US Patent 4,444,415, 1984.
8. Von der Ohe M. Front and rear suspension of the new model W201. SAE paper 831045, 1983, pp. 12.
9. Howard G. *Chassis and suspension engineering*. Oxford: Osprey Publishing, 1987.
10. Hespelt A and Von der Ohe M. *Independent wheel suspension for steerable wheels of motor vehicles*. US Patent 4,705,292, 1987.
11. Kubo K. *Vehicle suspension system for a steerable wheel*. US Patent 4,842,296, 1989.
12. Kubo K. *Vehicle suspension system for a steerable wheel*. US Patent 4,878,688, 1989.
13. Kami Y, Oku Y, Mizumoto K and Naka K. *Multi-link type suspension system*. US Patent 5,507,510, 1996.
14. Anon. 5-link double wishbone rear suspension development objectives. Report, Honda Worldwide, Tokyo, Japan,1997.
15. Lancia Dialogos, Lancia Thesis, Chrysler 300. Catalogs, Fiat Chrysler Automobiles, Turin, Italy 2000–2007.
16. Eppelein R. *Rear axle of a passenger vehicle with five individual links*. US Patent 7,048,286, 2006.
17. Amanos H. *Vehicular rear suspension system*. US Patent 7,258,355, 2007.
18. Ford Expedition and Expedition EL. Catalog, Ford Motor Company, Dearborn, Michigan, USA, 2012.
19. BMW Group. *Der neue BMW 7er: Entwicklung und Technik*. Berlin: Springer, 2009.
20. Okamoto K, Kajiwara H, Watanabe M and Mori M. *Suspension device*. US Patent 8,444,160, 2013.
21. Jung D, Lee J, Lee B and Kim S. The development of FR-Based 4WD multi-link suspension. SAE paper 2013-01-1235, 2013, pp. 8.
22. Lexus-GS, Lexus-ISF Lexus-LS. Catalogs, Toyota Motor Corporation, Nagoya, Japan, 2015.
23. Wildcat 4, Wildcat 1000. Catalogs, Arctic Cat Inc., Thief River Falls, Minnesota, USA, 2015.
24. Cadillac ATS Coupe. Catalog, General Motors Company, Detroit, Michigan, USA, 2015.
25. Anderson J, Bane O and Larsson A. Volvo 760 GLE multi-link rear axle suspension. SAE paper 890082, 1989, pp. 10.
26. Knable JJ and Nagreski DL. Design of a multilink independent front suspension for Class A motor homes. SAE paper 1999-01-3731, 1999, pp. 16.
27. Audi TT, Audi A3, Audi A4, Audi A6, Audi Q3. Catalogs, Audi AG, Ingolstadt, Germany, 2004–2015.
28. Lee U K, Lee S H, Jang HB and Park Y W. *Multi-link rear suspension system*. US Patent 7,243,934, 2007.
29. Porsche 911 GT2. Catalog, Porsche AG, Stuttgart, Baden-Württemberg, Germany, 2008.
30. Hirai H. *Vehicle suspension apparatus*. US Patent 7,798,507, 2010.
31. Chassis and suspension components. Catalog, Art Morrison Enterprises, Inc., Fife, Washington, USA, 2014.
32. Roth B. The kinematics of motion through finitely separated positions. *Trans ASME, J Appl Mech* 1967; 34: 591–598.
33. Roth B. Finite-position theory applied to mechanism synthesis. *Trans ASME, J Appl Mech* 1967; 34: 599–605.
34. Chen P and Roth B. Design equations for the finitely and infinitesimally separated position synthesis of binary links and combined link chains. *Trans ASME, J Engng Ind* 1969; 91(1): 209–219.
35. Sarkisyan YL, Gupta KC and Roth B. Spatial least square approximation of a given motion. In: *1st IFToMM international symposium on linkages and computer design methods*, Bucharest, Romania, 7–13 June 1973, Vol B, pp. 512–521.
36. Apetaur M. Zur kinematischen Synthese der Einzelradaufhängungen. *ATZ Automobiltechnische Z* 1975; 77(3): 85–88.
37. Suh CH. Synthesis and analysis of suspension mechanisms with use of displacement matrices. SAE paper 890098, 1989, pp. 12.
38. Raghavan M. Suspension kinematic structure for passive control of vehicle attitude. *Int J Veh Des* 1991; 12(5–6): 525–547.
39. Innocenti C. Polynomial solution of the spatial Burmester problem. *Trans ASME, J Mech Des* 1995; 117(1): 64–68.
40. Franchi CG, Migone F and Toso A. Genetic algorithms in multi-link front suspension optimization. In: *11th ADAMS European users' conference*, Frankfurt, Germany, 19–20 November 1996, pp. 1–16.
41. Raghavan M. Number and dimensional synthesis of independent suspension mechanisms. *Mechanism Mach Theory* 1996; 31(8): 1141–1153.
42. Simionescu PA. Kinematic synthesis and analysis of five-link rear wheel suspension system of automobiles. In: *7th IFToMM international congress on the theory of machines and mechanisms*, Liberec, Czech Republic, 3–5 September 1996, pp. 537–542.
43. Jimenez JM, Alvarez G, Cardenal J and Cuadrado J. A simple and general method for kinematic synthesis of spatial mechanisms. *Mechanism Mach Theory* 1997; 32(3): 323–341.

44. Kim SP, Shim JK and Lee TY. Approximate synthesis of 5-SS multi link suspension system using instantaneous screw axis. *KSME Int J* 1999; 25: 32–38.
45. Knapczyk J and Dzierzek S. Position–force synthesis of five-rod suspension mechanism. In: *10th IFToMM world congress on the theory of machines and mechanisms*, Oulu, Finland, 20–24 June 1999, Vol 2, pp. 671–676.
46. Alexandru C. Kinematic synthesis of the guiding mechanisms of the rear wheels of cars. In: *8th IFToMM international symposium on theory of machines and mechanisms*, Bucharest, Romania, 28 August–1 September 2001, Vol IV, pp. 1–6.
47. Bae S, Lee JM and Chu CN. Axiomatic design of automotive suspension systems. *Ann CIRP* 2001; 51(1): 115–118.
48. Kim S P, Shim J K, Ahn B E and Lee U K. Approximate synthesis of 5-SS multi link suspension system for steering motion. *KSME Int J* 2001; 25: 32–38.
49. Liao Q and McCarthy J M. On the seven position synthesis of a 5-SS platform linkage. *Trans ASME, J Mech Des* 2001; 123(1): 74–79.
50. Raghavan M. Suspension mechanism synthesis for linear toe curves. In: *ASME 2002 design engineering technical conferences and computer and information in engineering conference*, Montreal, Quebec, Canada, 29 September–2 October 2002, paper DETC2002/MECH-34305, pp. 5.
51. Simionescu PA and Beale DG. Synthesis and analysis of the five-link rear suspension system used in automobiles. *Mechanism Mach Theory* 2002; 37(9): 815–832.
52. Erratum. Synthesis and analysis of the five-link rear suspension system used in automobiles. *Mechanism Mach Theory* 2005; 40(12): 1414.
53. Knapczyk J and Maniowski M. Dimensional synthesis of a five-rod guiding mechanism for car front wheels. *Arch Mech Engng* 2003; 50(1): 89–116.
54. Figliolini G and Rea P. Synthesis and simulation of a multilink suspension mechanism. In: *9th IFToMM international symposium on theory of machines and mechanisms*, Bucharest, Romania, 1–4 September 2005, pp. 483–488.
55. Wach W and Struski J. Rear wheels multi-link suspension synthesis with the application of "virtual mechanism". SAE paper 2006-01-1376, 2006, pp. 12.
56. Struski J and Wach W. Multidimensional optimization of the steered wheel multi-link suspension system. SAE paper 2007-01-0849, 2007, pp. 9.
57. Lamers WJ. *Development and analysis of a multi-link suspension for racing applications*. Master's Thesis, Technische Universiteit Eindhoven, Eindhoven, The Netherlands, 2008.
58. Totu V and Alexandru C. Multi-criteria kinematic optimization of a front multi-link suspension mechanism using DOE screening and regression model. *Appl Mech Mater* 2013; 332: 351–356.
59. Angrosch B, Plöchl M and Reinalter W. Suspension design by means of numerical sensitivity analysis and optimization. *Int J Veh Des* 2014; 65(1): 52–72.
60. Sancibrian R, Garcia P, Viadero F and Fernandez A. Suspension system vehicle design using a local optimization procedure. In: *ASME 2005 international design engineering technical conferences and computers and information in engineering conference*, Long Beach, California, USA, 24–28 September 2005, paper DETC2005-84441, 10 pp.
61. Hiller M and Woernle C. Elasto-kinematical analysis of a five-point wheel suspension. *SIA Ing Auto, Paris* October 1985: 77–80.
62. Hiller M and Woernle C. Bewegungsanalyse einer fünfpunkt Radaufhangun. *ATZ Automobiltechnische Z* 1985; 87(2): 59–64.
63. Hiller M and Frik S. Road vehicle benchmark 2: five-link suspension. *Veh System Dynamics* 1993; 22(Suppl 1): 254–262.
64. Suh CH. Suspension analysis with instant screw axis theory. SAE paper 910017, 1991, pp. 9.
65. Knapczyk J and Dzierzek S. Displacement analysis of five-rod wheel-guiding mechanism by using vector method. In: *25th silver jubilee international symposium on automotive technology and automation*, Florence, Italy, 1–5 June 1992, pp. 687–695.
66. Hiller M. Five-link suspension. In: Kortüm W and Sharp RS (eds) *Multibody computer codes in vehicle system dynamics*. Amsterdam: Swets & Zeitlinger, 1993, pp. 254–262.
67. Knapczyk J and Dzierzek S. Effects of geometrical parameters and joint flexibilities on elasto-kinematic characteristics of five-rod rear wheel guide mechanisms. In: *6th IFToMM international symposium on the theory of machines and mechanisms*, Bucharest, Romania, 15 June 1993, Vol 4, pp. 83–90.
68. Lee DMA, Pascoe DM and El Maragy WH. An analysis of multilink independent suspension systems. *Int J Veh Des* 1993; 14(1): 44–58.
69. Unkoo L and Byeongeui A. Method to analyze the imaginary kingpin axis in multi-link type suspension systems. SAE paper 930262, 1993, pp. 18.
70. Hiller M. Five-point wheel suspension. In: Angeles J and Kecskemethy A (ed) *Kinematics and dynamics of multi-body systems*. Berlin: Springer, 1995, pp. 177–188.
71. Knapczyk J and Dzierzek S. Displacement and force analysis of five-rod suspension with flexible joints. *Trans ASME, J Mech Des* 1995; 117(4): 532–538.
72. Mohamed MG and Attia H A. Numerical kinematic analysis of the motor-vehicle multilink suspension system. In: *1995 ASME design engineering technical conferences, 21th ASME design automation conference*, Boston, Massachusetts, USA, 17–20 September 1995, pp. 883–889.
73. Knapczyk J and Dzierzek S. Elastokinematic analysis of the five rod suspension considering joint elasticities. In: *9th IFToMM world congress on the theory of machines and mechanisms*, Milan, Italy, 29 August–5 September 1995, Vol 4, pp. 2824–2828.
74. Attia HA. Dynamic analysis of the multi-link five-point suspension system using point and joint coordinates. *Acta Mech* 1996; 119: 221–228.
75. Cambiaghi D, Gadola M, Vetturi D and Manzo L. Multi-link suspension analysis: an elastokinematic model. In: *29th international symposium on automotive technology and automation*, Florence, Italy, 3–6 June 1996, paper 96VR031.
76. Merlet JP. Kinematic analysis of a rear suspension. In: *International symposium on automotive technology and automation*, Florence, Italy, 3–6 June 1996, pp. 8.
77. Simeon B. On the numerical solution of a wheel suspension benchmark problem. *J Comput Appl Math* 1996; 66(1–2): 443–456.

78. Knapczyk J and Dzierzek S. Elastokinematic analysis of five-rod suspension with flexible joints, including effects of shock absorber. *Veh System Dynamics* 1998; 29(1): 270–279.
79. Candelpergher A, Gadola M and Vetturi D. Development of a new software for racecar suspension kinematics. SAE paper 2002-01-3346, 2002, pp. 8.
80. Rocca E and Russo R. A feasibility study on elastokinematic parameter identification for a multilink suspension. *Proc IMechE Part D: J Automobile Engineering* 2002; 216(2): 153–160.
81. Attia HA. Kinematic analysis of the multi-link five-point suspension system in point coordinates. *KSME Int J* 2003;17(8): 1133–1139.
82. Knapczyk J and Maniowski M. Elastokinematic modeling and study of five-rod suspension with subframe. *Mechanism Mach Theory* 2006; 41(9): 1031–1047.
83. Knapczyk J and Maniowski M. Stiffness synthesis of a five-rod suspension for given load–displacement characteristics. *Proc IMechE Part D: J Automobile Engineering* 2006; 220(7): 879–889.
84. Wang X-L, Dai L and Shangguan WB. Calculation of joint forces of a multilink suspension for strength and fatigue analysis of bushings and control arms. *Int J Veh Des* 2014; 66(3): 217–234.
85. Qiu C, Zhang K, Zhao JS and Dai JS. Stiffness design, analysis and validation of a parallel mechanism equivalent suspension system. In: *ASME 2015 international design engineering technical conferences and computers and information in engineering conference*, Boston, Massachusetts, USA, 2–5 August 2015, paper DETC2015-46641, 11 pp.
86. Li L, Xia C and Qin W. Analysis of kinetic characteristic and structural parameter optimization of multi-link suspension. SAE paper 2007-01-3558, 2007, pp. 5.
87. Heo JH, Lee UK and Lee SH. Development of a method to compute the kingpin axis using screw axis theory based on suspension-parameter-measuring device data. *Proc IMechE Part D: J Automobile Engineering* 2009; 233(4): 519–531.
88. Balike P. *Kineto-dynamic analyses of vehicle suspension for optimal synthesis*. PhD Dissertation, Concordia University, Montreal, Quebec, Canada, 2010.
89. Uchida T and McPhee J. Efficient solution of kinematics for multi-loop mechanisms using Gröbner bases. In: *13th IFToMM world congress in mechanism and machine science*, Guanajuato, Mexico, 19–25 June 2011, paper IMD-123, pp. 1–9.
90. Uchida T and McPhee J. Using Gröbner bases to generate efficient kinematic solutions for the dynamic simulation of multi-loop mechanisms. *Mechanism Mach Theory* 2012; 52: 144–157.
91. Suh CH. Design of space mechanisms for rigid body guidance. *Trans ASME, J Mfg Sci Engng* 1968; 90(3): 499–506.
92. Suh CH and Radcliffe CW. *Kinematics and mechanisms design*. New York: John Wiley, 1978.
93. Sandor GN, Kohli D and Zhuang X. Synthesis of RSSR-SRR spatial motion generator mechanism with prescribed crank rotations for three and four finite positions. *Mechanism Mach Theory* 1985; 20(6): 503–519.
94. Sandor GN, Xu LJ and Yang SP. Computer aided synthesis of two-closed loop RSSR-SS spatial motion generators with branching and sequence constraints. *Mechanism Mach Theory* 1986; 21(4): 345–350.
95. Premkumar P and Kramer S. Synthesis of multi-loop spatial mechanisms by iterative analysis: the RSSR−SS path generator. *Trans ASME, J Mech Des* 1990; 112(2): 69–73.
96. Sincere SM. Short–long arm suspension system nonlinearities and analysis. SAE paper 983033, 1998, pp. 8.
97. Esat I. Genetic algorithm-based optimization of a vehicle suspension system. *Int J Veh Des* 1999; 21(2–3): 148–160.
98. Attia HA. Numerical kinematic analysis of the double wishbone motor-vehicle suspension system. *Trans Can Soc Mech Engrs* 2000; 24(2): 391–399.
99. Attia HA. Dynamic modeling of the double wishbone motor-vehicle suspension system.European *J. Mech A/Solids* 2002; 21(1): 167–174.
100. Bian X, Song BA and Walter R. Optimization of steering linkage and double-wishbone suspension via R-W multi-body dynamic analysis. *Forsch Ingenieurwesen* 2004; 69: 38–43.
101. Raghavan M. Suspension synthesis for *N*:1 roll center motion. *Trans ASME, J Mech Des* 2005; 127(4): 673–678.
102. Hwang JS, Kim SR and Han SY. Kinematic design of a double-wishbone type front suspension mechanism using multi-objective optimization. In: *5th Australasian congress on applied mechanics*, Brisbane, Australia, 10–12 December 2007. 6 pages
103. Arikere A, Kumar GS and Bandyopadhyay S. Optimization of double wishbone suspension system using multi-objective genetic algorithm. In: Simulated Evolution and Learning, Lecture Notes in Computer Science, Berlin: Springer, (2010) p.445–454.
104. Sancibrian R, Garcia P, Viadero F et al. Kinematic design of double-wishbone suspension systems using a multiobjective optimization approach. *Veh System Dynamics* 2010; 48(7): 793–813.
105. Wang Y, Gao JQ and Chen E. Kinematic analysis and optimum design of double wishbone independent suspension based on Adams/View. *Advd Mater Res* 2011; 314–316: 2091–2095.
106. Liang J and Xin L. Simulation analysis and optimization design of front suspension based on Adams. *Mechanika* 2012; 18(3): 337–340.
107. Shen Q, Russell K and Sodhi RS. Analytical displacement and velocity modeling of the RSSR-SS linkage. *Adv Mechanisms Des, Mechanisms Mach Sci* 2012; 8: 151–156.
108. Liu X, Luo J, Wang Y et al. Analysis for suspension hardpoint of Formula SAE car based on correlation theory. *Res J Appl Sci, Engng Technol* 2013; 6(24): 4569–4574.
109. Russell K, Shen Q and Sodhi RS. *Mechanism design: visual and programmable approaches*. Boca Raton, Florida: CRC Press, 2014.
110. Wu J, Luo Z, Zhang Y and Zhang N. An interval uncertain optimization method for vehicle suspensions using Chebyshev metamodels. *Appl Mathl Modelling* 2014; 38: 3706–3723.
111. Cheng X and Lin Y. Multiobjective robust design of the double wishbone suspension system based on particle swarm optimization. *Scient World J* 2014: Article ID 354857, pp. 7.
112. Shen Q, Lee W-T and Russell K. A small-scale optimization model for RSSR-SS motion generation with branch and order defect elimination in Matlab, Journal

of Advanced Mechanical Design, Systems, and Manufacturing, 8(3), 2014, pp. 8.
113. Atashrazm R. *Topology based optimization of suspension and steering mechanisms of automobiles*. MS Thesis, University of Waterloo, Waterloo, Ontario, Canada, 2015.
114. Tanik E. and Parlaktaş V. On the analysis of double wishbone suspension regarding steering input and anti-dive/lift effect, Journal of Advanced Mechanical Design, Systems, and Manufacturing, 10(2), 2016, pp. 11.
115. Uberti S, Gadola M, Chindamo D, Romano M and Galli F. Design of a double wishbone front suspension for an orchard–vineyard tractor: Kinematic analysis, Journal of Terramechanics, 57, (2015), p. 23–39.
116. Pressnell J. *Citroën Traction Avant*. Ramsbury, Wiltshire: Crowood Press, 2006.
117. Slack FW. *Automobile suspension system*. US Patent 2,063,704, 1936.
118. Crane HM. *Automobile suspension system*. US Patent 2,027,577, 1935.
119. Slack FW. *Vehicle wheel connecting joint*. US Patent 2,405,458, 1946.
120. Bastow D. Suspension and steering. *Auto Engr* 1968; 10: 221–232.
121. Kami Y and Minikawa M. Double-wishbone suspension for Honda Prelude. SAE paper 841186, 1984, pp. 10.
122. Topaç MM, Deryal U, Bahar E and Yavuz G. Optimal kinematic design of a multi-link steering system for a bus independent suspension: an application of response surface methodology. *Mechanika* 2015; 21(5): 404–413.
123. Axle systems for coaches. Catalog, ZF Industries, Inc., Division Commercial Vehicle Technology, Vernon Hills, Illinois, USA, 2014.
124. Independent front suspension for heavy-duty trucks. Catalog, ZF Industries, Inc., Division Commercial Vehicle Technology, Passau, Germany, 2014.
125. Bowman DA, Schafer CA, Jeffries LD and Brown JK. *Tractor with front suspension*. US Patent 6,470,991, 2002.
126. Fendt tractors. Catalog, AGCO Corp., Duluth, Georgia, USA, 2014.
127. HMMWV. Catalog, AM General LLC, South Bend, Indiana, USA, 1984–2015.
128. John Deere Gator utility vehicles. Catalog, Deere & Company, Moline, Illinois, USA, 2015.
129. Tanahashi H. *Vehicle rear wheel suspension with dual links extending in the overall forward direction*. US Patent 4,650,211, 1987.
130. Koide R, Kawabe Y, Nakajima K and Kazuhiro K. Development of a new multi-link rear suspension. SAE paper 2012-01-0978, 2012.
131. Koide R, Nakajima K and Kawabe Y. *Suspension structure and link arranging method*. US Patent 8,678,409, 2014.
132. Kami K, Minakawa M and Kubo K. *Suspension for vehicles*. US Patent 4,538,831, 1985.
133. Iijima Y and Noguchi H. The development of a high-performance suspension for the new Nissan 300ZX. SAE Paper 841189, 1984, pp. 12.
134. Higuchi A. *Suspension of a vehicle*. US Patent 4,844,505, 1989.
135. Murakami T. *Double link type suspension including a stabilizer bar*. US Patent 4,875,703, 1989.
136. Tsukuda Y, Tsubota Y, Tonomura H and Naguchi H. Development of a new multi-link rear suspension. SAE paper 881774, 1988, pp. 10.
137. Murakami T, Uno T, Iwasaki H and Noguchi H. Development of a new multi-link front suspension. SAE paper 890179, 1989, pp. 10.
138. Ushio K. New multi-link suspension. SAE paper 912567, 1991, pp. 11.
139. Lee U. *Suspension system for vehicle*. US Patent 5,560,637, 1996.
140. Lee U. *Vehicle suspension system for a steerable wheel*. US Patent 5,346,241, 1994.
141. Lee U. *Suspension system for front wheel of a vehicle*. US Patent 5,697,633, 1997.
142. Fujita K, Hirokawa N, Akagi S and Hirata T. Design optimization of multi-link suspension system for total vehicle handling and stability. In: *7th AIAA/USAF/NASA/ISSMO symposium on multidisciplinary analysis and optimization*, St Louis, Missouri, 2–4 September 1998, paper AIAA-98-4787, pp. 620–631.
143. Kasahara T, Morioka N, Satou M et al. Development of a new multi-link suspension. SAE paper 2000-01-0092, 2000, pp. 10.
144. Simionescu PA and Smith MR. Initial estimates in the design of rack-and-pinion steering linkages. *Trans ASME, J Mech Des* 2000; 122(2): 194–200.
145. King-Hele D. Erasmus Darwin's improved design for steering carriages and cars. *Notes Rec R Soc Lond* 2002; 56(1): 41–62.
146. Simionescu PA, Smith MR and Tempea I. Synthesis and analysis of the two loop translational input steering mechanism. *Mechanism Mach Theory* 2000; 35(7): 927–943.
147. Tsai LW. *Robot analysis: the mechanics of serial and parallel manipulators*. New York: John Wiley, 1999.
148. Simionescu PA. *Computer aided graphing and simulation tools for AutoCAD users*. Boca Raton, Florida: CRC Press, 2014.
149. Simionescu PA. Animated GIF's of 5-link, 4-link and 3-link suspension mechanisms with rack and pinion steering control, www.researchgate.net/publication/290604178_GIF_files_1 (2016).